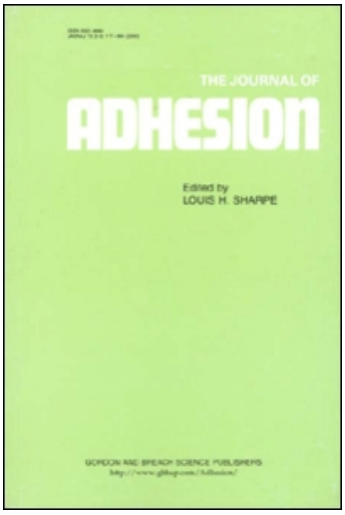


**The Journal of Adhesion**
Publication details, including instructions for authors and subscription information:
http://www.informaworld.com/smpp/title~content=t713453635

# Compressive Fiber Fragmentation in Carbon/Polypropylene Composites: Effects of Residual Thermal Stresses and Transcrystallinity

A. Gáti[a]; H. D. Wagner[a]
[a] Department of Materials and Interfaces, The Weizmann Institute of Science, Israel

**To cite this Article** Gáti, A. and Wagner, H. D.(1996) 'Compressive Fiber Fragmentation in Carbon/Polypropylene Composites: Effects of Residual Thermal Stresses and Transcrystallinity', The Journal of Adhesion, 58: 1, 25 — 42
**To link to this Article: DOI:** 10.1080/00218469608014398
**URL:** http://dx.doi.org/10.1080/00218469608014398

*J. Adhesion*, 1996, Vol. 58, pp. 25–42
Reprints available directly from the publisher
Photocopying permitted by license only



# Compressive Fiber Fragmentation in Carbon/Polypropylene Composites: Effects of Residual Thermal Stresses and Transcrystallinity*

A. GÁTI and H. D. WAGNER**

*Department of Materials and Interfaces, The Weizmann Institute of Science, Rehovot 76100, Israel*

*(Received February 10, 1995; in final form July 17, 1995)*



The effects of fiber volume fraction and transcrystallinity in single fiber composites, on the phenomenon of compressive fiber fragmentation due to residual thermal stresses, are studied. A concentric cylinder model is used, jointly with experimental data, to predict the Weibull shape parameter of the compressive strength distribution of pitch-based high and medium modulus (HM and MM) carbon fibers, with isotactic polypropylene as the semi-crystalline embedding matrix. A severe effect of the fiber content on the thermal residual stress in the fiber and, thus, on the fiber break density, is predicted and experimentally confirmed. The effect of the presence of isothermally grown polypropylene transcrystalline interlayers (using pitch-based HM carbon fibers as a substrate) on the compressive stresses induced upon subsequent quenching is investigated, both experimentally and theoretically. Cooling rate results are also presented. The thermoelastic constants of the interlayer are predicted to have a severe effect on the residual stresses generated in the fiber, the interphase, and the matrix. There is therefore, a definite need for direct experimental measurements of these constants.

KEY WORDS: Residual thermal stress; single fiber composites; compressive fragmentation; Weibull shape parameter; transcrystalline interlayer; effect of thickness; fiber volume fraction; concentric cylinder model; isotactic polypropylene; interphase; theory; experiment.

## 1. INTRODUCTION

The interface, or interlayer, between reinforcing fibers and matrix is widely regarded as an important factor in determining the mechanical properties of composite materials. Much information about the interface can be gained by investigating single fiber composites (SFCs), which are essentially model composites in which a limited number of single fibers are embedded in a matrix film. Changes in matrix morphology around the fiber may affect the fiber/matrix adhesion. For example, the formation of a transcrystalline layer might possibly influence the mechanical properties of the fiber/matrix interface, and of the composite, in currently unknown ways. Single fiber composite tests, such as the fragmentation test, are used to estimate the adhesion

* One of a Collection of papers honoring Jacques Schultz, the recipient in February 1995 of *The Adhesion Society Award for Excellence in Adhesion Science, Sponsored by 3M.*

** Corresponding author.

between a rigid fiber and a more ductile polymer matrix.[1,2] A parameter that reflects the extent of the adhesion is the interfacial shear strength (ISS), $\tau$, and different authors have used different approaches for the calculation of the stress state at the interface. The prevailing models are those of Kelly and Tyson[3] (KT), and Cox.[4] A key variable in the KT model is the tensile strength of a small fiber fragment length, and residual thermal stresses in the fiber prior to testing are usually neglected in the calculations. However, recent experiments in our laboratory with pitch-based high modulus (HM) and medium modulus (MM) carbon/polypropylene SFCs, show that compressive fiber fragmentation occurs during sample preparation. This "spontaneous" fiber fragmentation is attributed to residual thermal stresses.

In this paper we calculate the residual thermal stresses present in SFCs, and utilize this calculation, and generate compressive fiber fragmentation data, to estimate the (compressive) strength and Weibull shape parameter of the embedded fiber. In addition, the effect of the presence of isothermally grown polypropylene transcrystalline interlayers (using pitch-based HM carbon fibers as a substrate) on the compressive stresses induced upon subsequent quenching is investigated, both experimentally and theoretically.



## 2. EXPERIMENTAL

Sample preparation was identical for both HM and MM single fiber composite samples. Films of isotactic polypropylene (iPP) (Exxon Corporation, MFR = 12) were prepared in a small laboratory press (Carver Inc). Their thickness varied between 100 and 300 μm. A single 20 mm long, 10 μm diameter, pitch-based carbon fiber (PRD-172 from E. I. du Pont de Nemours, Inc.) was sandwiched between rectangular strips ($20 \times 5\,mm^2$) previously cut out from the polypropylene films. Varying the fiber volume fraction was achieved by laying different amounts of single fibers between similar polypropylene strips, in an approximately parallel array. The fiber-to-fiber distance was never less than about ten fiber diameters. Fiber volume fractions were calculated based on visual observation under the microscope, and accounting for the measured thickness of each individual sample. There was no statistically-significant difference between film thickness for samples of differing volume fractions. Samples, covered with a thin glass cover, were then placed on a thick microscope slide and inside a Mettler FP90 hot stage apparatus (Fig. 1). The following heating/cooling cycles were used:

*i) HM carbon fiber reinforced iPP.* These samples were first heated to 204°C for 3 minutes in order to erase any memory of the polymer and then either (a) cooled to an isothermal temperature of 131°C, to allow nucleation and growth of the transcrystalline layer, followed by quenching down to 0°C, or (b) cooled to room temperature at rates ranging from 0.3°C $min^{-1}$ to 400°C $min^{-1}$, or (c) in the study of fiber volume fraction effects, quenched directly to 0°C. The nucleation and growth of an iPP transcrystalline layer onto a HM graphite fiber is depicted in Figure 2, using polarized light microscopy. As seen, at 131°C a large iPP transcrystalline region (radius of about 120 μm) may be grown from the surface of HM graphite in about 25 minutes.

*ii) MM carbon fiber reinforced iPP.* After 3 minutes at 204°C these samples were quenched to −196°C (liquid $N_2$ temperature), rather than to 0°C as in the case of HM

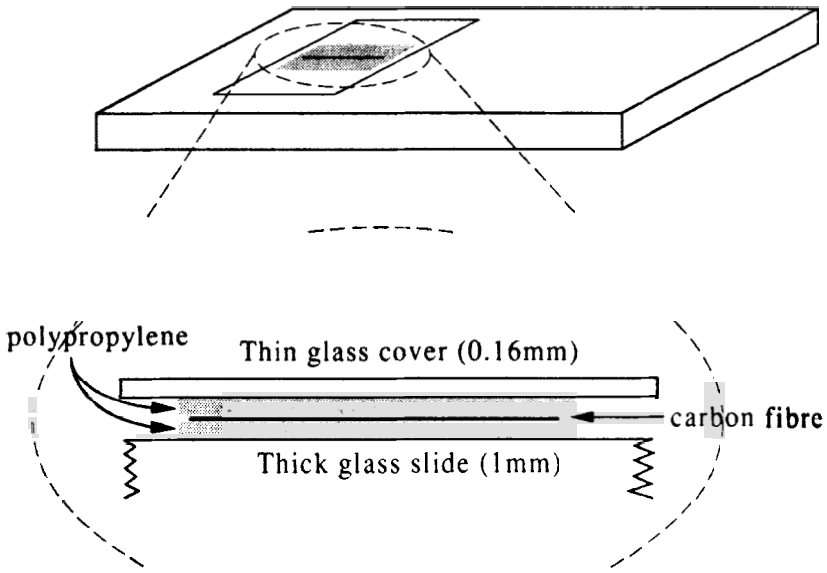


FIGURE 1 Schematic description of the sample preparation procedure.



fiber composite samples. Indeed, the MM fibers being not as brittle as the HM fibers, a larger temperature drop ensured sufficient break density for the length of samples that were used. We did not observe nucleation of a transcrystalline interphase on MM carbon surfaces; however, this system could still be utilized to study the effect of fiber volume fraction on the compressive stresses present in the fiber during quenching.

The density of compressive breaks was measured for all samples. Using optical microscopy the compressive breaks were identified more easily by shining light onto the samples from both sides of the microscope, together with conventionally transmitted light (Fig. 3). Ideally, fiber break density should be monitored during sample cooling. However, this proved difficult in practice because the sample inside the hot stage can be viewed only through a small pinhole, the size and depth of which make it impossible for the sample to be illuminated from the sides of the microscope. Thus, the technique described in Figure 3 can be used only when the sample is outside the hot stage.

## 3. THEORY

In this section theoretical expressions are presented for the principal stresses in the fiber, matrix and the interlayer between them, due to the residual thermal stresses resulting from specimen preparation at a relatively high reference temperature. Mainly, we focus on the two-concentric-cylinder model of Nairn[5] where both cylinders are assumed to be transversely isotropic and the interface is infinitely thin (Fig. 4a). When a transcrystalline interlayer exists, a similar three-cylinder model[5-8] may be used (Fig. 4b). The cylinder radii for the fiber and the interlayer are $R_1$ and $R_2$, respectively. The equivalent

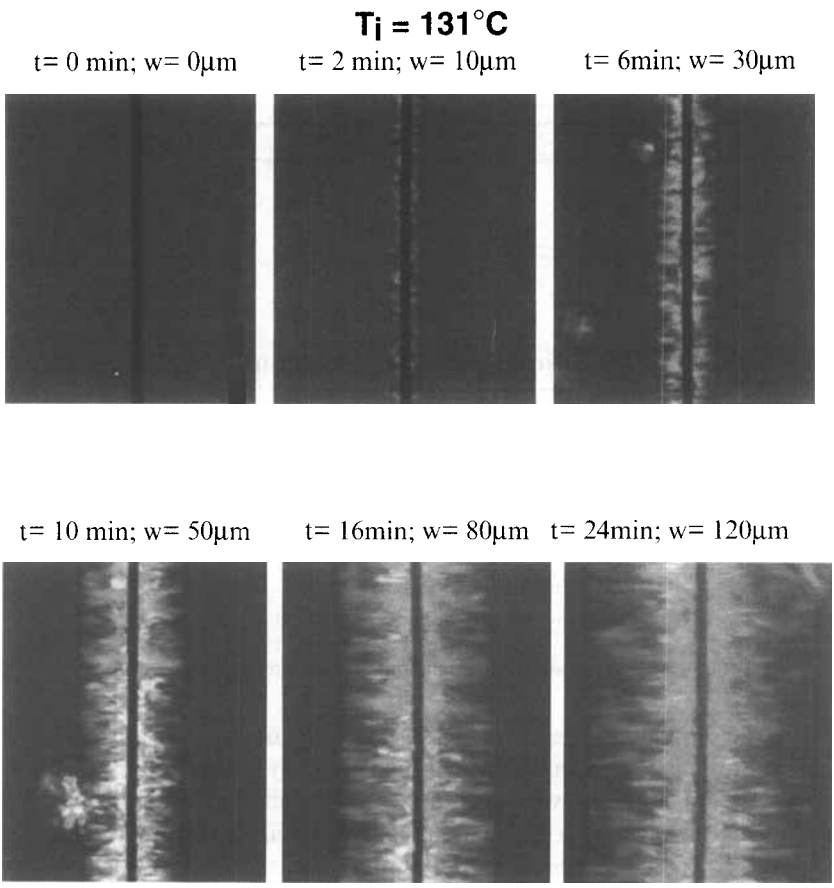




FIGURE 2 Nucleation and growth of a transcrystalline layer from a HM carbon fibre surface, at $T_i = 131$ °C isotherm. The sequence of photographs, taken using polarised light microscopy, demonstrates the rate of transcrystalline growth. The fiber diameter is 10 μm. (See Color Plate I).

matrix radius, $R_3$, was determined by equating the rectangular cross sectional area of the sample with an equivalent circular cross sectional area. Thus, $R_1 = 5$ μm (the radius of the carbon fiber), $R_2$ varies between 0 and 100 μm, and $R_3 = 690$ μm.

### 3.1 The Two-Cylinder Model

Following Lekhnitskii,[9] and including thermal strain effects, the stress-strain relationship for transversely isotropic materials takes the following form (in cylindrical coordinates):

$$\begin{pmatrix} \varepsilon_{rr} \\ \varepsilon_{\theta\theta} \\ \varepsilon_{zz} \end{pmatrix} = \begin{pmatrix} \frac{1}{E_r} & -\frac{\nu_{\theta r}}{E_r} & -\frac{\nu_{zr}}{E_z} \\ -\frac{\nu_{\theta r}}{E_r} & \frac{1}{E_r} & -\frac{\nu_{zr}}{E_z} \\ \frac{\nu_{zr}}{E_z} & -\frac{\nu_{zr}}{E_z} & \frac{1}{E_z} \end{pmatrix} \begin{pmatrix} \sigma_{rr} \\ \sigma_{\theta\theta} \\ \sigma_{zz} \end{pmatrix} + \begin{pmatrix} \alpha_r \\ \alpha_r \\ \alpha_z \end{pmatrix} \Delta T \tag{1}$$

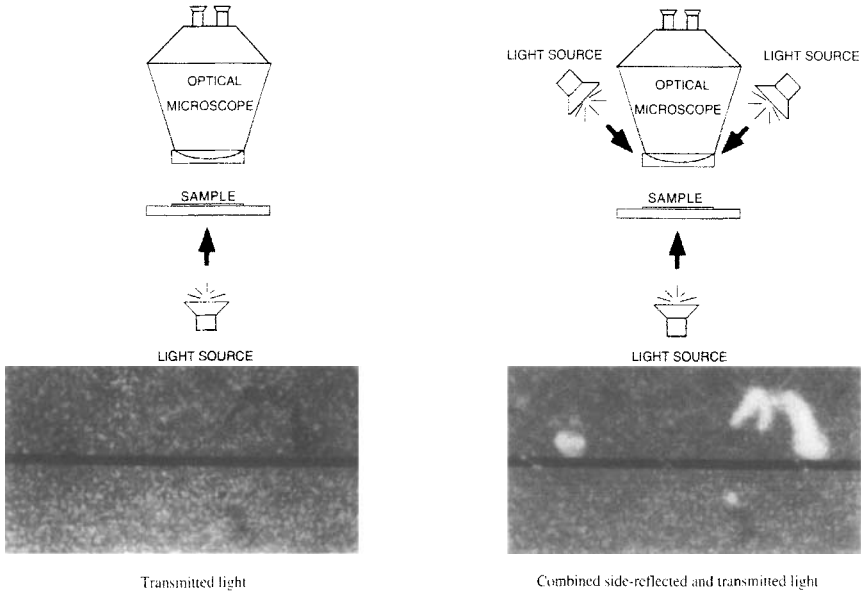


FIGURE 3 Improved viewing technique for the observation of compressive breaks. (See Color Plate II)



where $\sigma$- and $\varepsilon$ designate stress and strain, respectively, $\alpha$ is the thermal expansion coefficient, $\nu$ and $E$ are the Poisson's ratio and Young's modulus, and $\Delta T = T - T_{ref}$, where $T_{ref}$ is a reference temperature. As seen, there are four independent elastic constants and two thermal expansion coefficients. Using classical elasticity methods, the stresses in the fiber and the matrix can be reduced to the determination of 5 constants $A^f$, $C^f$, $A^m$, $B^m$, and $C^m$, each of which is expressed in terms of the materials elastic constants, the thermal expansion coefficients, $\Delta T$, and the fiber volume fraction (details of the procedure can be found in References 5–7).

For the fiber this results in

$$\sigma_{rr}^f = \sigma_{\theta\theta}^f = A^f \tag{2}$$

$$\sigma_{zz}^f = C^f \tag{3}$$

and for the matrix

$$\sigma_{rr}^m = A^m + B^m\left(\frac{R_1}{r}\right)^2 \tag{4}$$

$$\sigma_{\theta\theta}^m = A^m - B^m\left(\frac{R_1}{r}\right)^2 \tag{5}$$

$$\sigma_{zz}^m = C^m \tag{6}$$

where the superscripts $f$ and $m$ designate the fiber and matrix, respectively, and $r$ is the radial coordinate. The next steps in the analysis involve radial stress boundary conditions associated with continuity of tractions at interfaces, and a force balance in

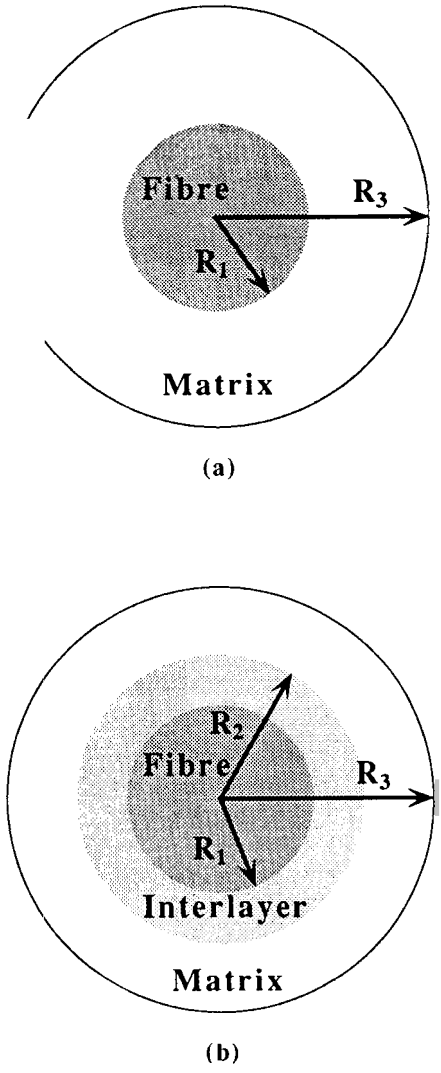




FIGURE 4 The concentric cylinder model, as a schematic representation of the cross section of single fiber composites: (a) without interlayer and (b) with interlayer. Throughout this work $R_1$ and $R_3$ had values of 5 μm and 690 μm, respectively, and $R_2$ was varied between 0 and 100 microns.

the longitudinal direction,[5-7] from which it can be shown that the number of unknowns may be reduced to two, namely, $A^m$ and $C^m$. These can then be determined by applying the stress-strain relations (Eq. 1) with interfacial no-slip conditions, which yields two simultaneous equations with the above two unknowns. The simultaneous equations are solved and the residual thermal stresses in both the fiber and the matrix are determined from Eqs. (2–6). The longitudinal compressive stress in the fiber is found to be the largest of all the stresses in both the fiber and the matrix. Details can be found in References 5–7.

### 3.2 The Three-Cylinder Model

The analysis is essentially the same as for the two-cylinder case. The form of the stress components is as follows:

For the fiber:

$$\sigma_{rr}^f = \sigma_{\theta\theta}^f = A^f \tag{7}$$

$$\sigma_{zz}^f = C^f \tag{8}$$

For the interlayer:

$$\sigma_{rr}^i = A^i + B^i\left(\frac{R_2}{r}\right)^2 \tag{9}$$

$$\sigma_{\theta\theta}^i = A^i - B^i\left(\frac{R_2}{r}\right)^2 \tag{10}$$

$$\sigma_{zz}^i = C^i \tag{11}$$

For the matrix:

$$\sigma_{rr}^m = A^m + \frac{B^m}{r^2} \tag{12}$$

$$\sigma_{\theta\theta}^m = A^m - \frac{B^m}{r^2} \tag{13}$$

$$\sigma_{zz}^m = C^m \tag{14}$$

Here we have eight unknown parameters, namely, $A^f, C^f, A^i, B^i, C^i, A^m, B^m$, and $C^m$. By inserting boundary conditions and using a force balance analysis in the longitudinal direction, these reduce to only four unknown parameters, namely, $A^m, C^m, B^i$, and $C^i$, which again are expressed in terms of the materials elastic constants, the thermal expansion coefficients, $\Delta T$, and the fiber volume fraction. The residual thermal stresses in the phases may then be determined as in the 2-cylinder case, see details elsewhere.[5-7]

## 4. RESULTS AND DISCUSSION

### 4.1 Fiber Properties in Compression: Axial Residual Stress, Number of Breaks, and Weibull Shape Parameter

The effect of the fiber volume fraction on the longitudinal compressive stresses in the fiber was studied both theoretically (using the analysis of the previous section), and experimentally. Theoretical results are described in Figure 5, using the data in Table I. For HM carbon in polypropylene, the value of $\Delta T$ was $-130°C$ (the difference between the isothermal crystallisation temperature, 130°C, and iced water, 0°C). Since the samples were cooled very fast (a few seconds over the previously mentioned temperature range) and since viewing of the breaks during cooling proved difficult, as mentioned earlier, it was assumed that the breaks were induced at the lowest temperature, although this is not known. The fiber longitudinal compressive stress is found to

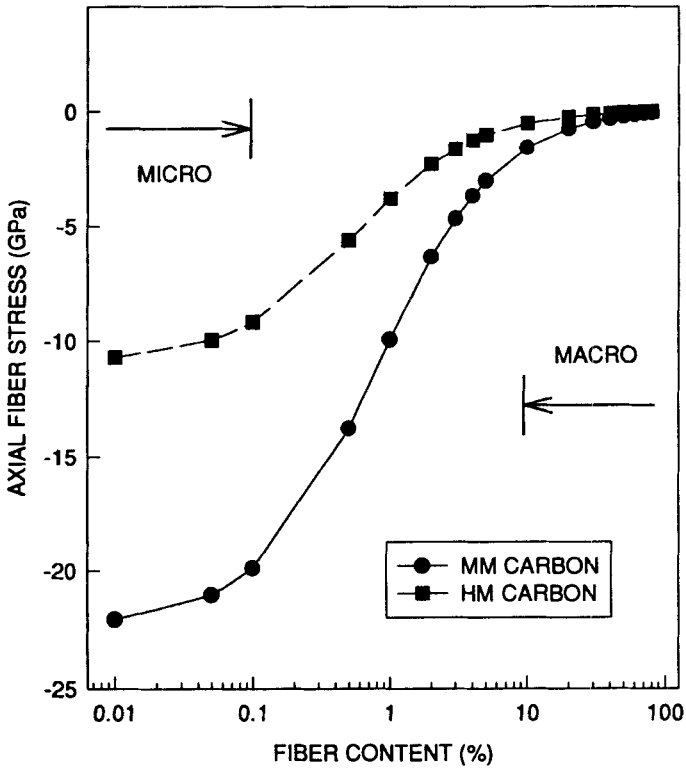


FIGURE 5 Calculated longitudinal stress in the fiber as a function of fiber volume fraction for HM and MM carbon/polypropylene composites.



TABLE I
Thermomechanical data for the fiber, matrix and transcrystalline interlayer

| Thermoelastic Constants | Fiber carbon HM | Fiber carbon MM | Matrix polypropylene (spherulitic) | Interphase polypropylene (transcrystalline) case 1 | Interphase polypropylene (transcrystalline) case 2 |
|---|---|---|---|---|---|
| Young's modulus $E_z$[GPa] | 750 | 500 | 4 | 80 | 8 |
| Young's modulus $E_r$ [GPa] | 15 | 20 | 4 | 8 | 80 |
| Poisson's ratio $\nu_{zr}$ | 0.22 | 0.25 | 0.3 | 0.2 | 0.2 |
| Poisson's ratio $J_{\theta r}$ | 0.25 | 0.1 | 0.3 | 0.35 | 0.35 |
| Thermal expansion coefficient $\alpha_z[10^{-6}°C^{-1}]$ | − 1.50 | − 1.48 | 110 | 10 | 10 |
| Thermal expansion coefficient $\alpha_r[10^{-6}°C^{-1}]$ | 10 | 12.4 | 110 | 50 | 50 |

be much larger than the other fiber stresses and is, therefore, considered to be the stress responsible for fiber fragmentation.

The presence of glass slides around the carbon/iPP composites was not taken into account here. The relative volume content of PP is about 0.15–0.20 (with respect to the glass slide/PP/glass slide laminate). This might suggest that the stress due to glass slide cooling overwhelms all others stresses present. This, we argue, was not the case: A variation in fiber break density at different fiber volume fractions *was* observed, even though the effect of the glass slides was kept as a constant parameter throughout the experiments. Thus, it was concluded that the strong decrease in the fiber break density with increasing fiber content could not result from the presence of (or any effect due to) the sandwiching slides.

A significant increase in the longitudinal stress is predicted (Fig. 5) when passing from high fiber volume fraction (*i.e.* real composite materials) to low fiber volume fraction (*i.e.* microcomposites). As seen, the fiber stress may become very large (up to $\sim 12$ GPa or $\sim 100{,}000$ atmospheres); for microcomposites, such as the ones used in our experiments (for which fiber volume percent is between 0.1 and 0.01), there is a significant variation in the compressive stress as a function of fiber volume percent. Similarly, for MM carbon in polypropylene, using $\Delta T = -400°C$ (remembering that these specimens were quenched from 204°C down to liquid nitrogen temperature, $-196°C$), a very large increase in the longitudinal compressive fiber stress is predicted at decreasing fiber volume fraction, refer to Figure 5. [Note that the theory predicts that *under the same* $\Delta T$, the compressive stress is much higher in a HM fiber than in a MM fiber; however, here, for the HM and the MM fibers we have used $\Delta T = -130$ C and $-400$ C, respectively, which explains why Fig. 5 shows much larger compressive stresses in the MM fiber than in the HM fiber].

The trend of these predictions was confirmed experimentally. For example, using HM carbon fibers in polypropylene, the number of compressive breaks per unit length of fiber was found to be smaller at higher volume fractions (Fig. 6). The much lower density of breaks, observed at higher volume fraction, indicates a smaller thermal residual stress in the fiber. The experimental variation in the fiber volume fraction could not be made to span the full range from a microcomposite to a real-life macrocomposite: the volume fraction was increased by slightly more than one order of magnitude, which was enough, nevertheless, to demonstrate the associated decrease in the fiber residual compressive stress. Regarding MM carbon in polypropylene, the number of observed compressive breaks per unit length was found to be comparatively smaller (due to the lower Young's modulus of the fiber) and sine-waving was also sometimes observed, another piece of evidence for large stresses induced upon cooling.

The number of compressive breaks can be predicted as a function of the temperature drop, if we assume that the fiber *compressive* strength follows a two-parameter Weibull distribution, as is commonly done with *tensile* strength. The ratio of average compressive strengths of two fibers with lengths $L_1$ and $L_2$ is given by:[6,10]

$$\frac{\langle \sigma \rangle_{L_1}}{\langle \sigma \rangle_{L_2}} = \left( \frac{L_1}{L_2} \right)^{-1/\beta} \tag{15}$$

which, as seen, depends on the (compressive) Weibull shape parameter of the fiber. Eq. (15) can be rewritten in terms of the number of breaks ($N_1$ and $N_2$) per unit length of

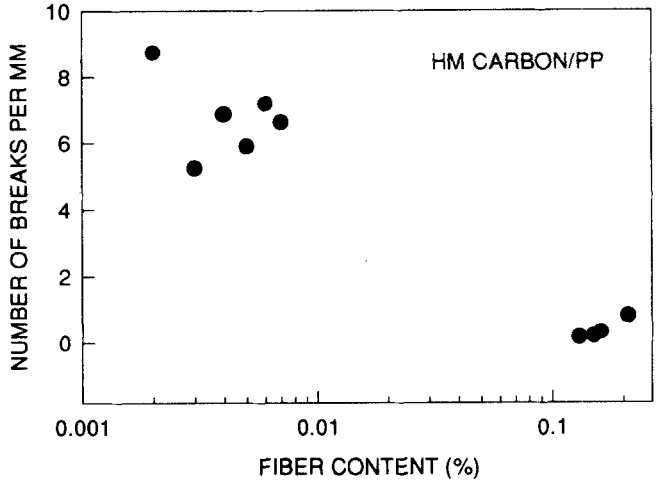


FIGURE 6 Number of breaks per unit length of fiber as a function of fiber volume fraction for HM carbon fibers in a polypropylene matrix.



fiber. If $L_0$ is the original fiber gauge length, substituting $L_1 = L_0/N_1$ and $L_2 = L_0/N_2$ into Eq. (15), we obtain for two fibers fragments of lengths $L_1$ and $L_2$:

$$\frac{\langle\sigma\rangle_{L_1}}{\langle\sigma\rangle_{L_2}} = \left(\frac{N_2}{N_1}\right)^{-1/\beta}. \tag{16}$$

In particular, when $L_1 = L_0$, we have $N_1 = 1$ and the density of breaks up to a stress level $\langle\sigma\rangle_{L_i}$, is given by:

$$N_i = \left(\frac{\langle\sigma\rangle_{L_0}}{\langle\sigma\rangle_{L_i}}\right)^{-\beta}. \tag{17}$$

Therefore, to predict the number of breaks, $N_i$, up to a stress level, $\langle\sigma\rangle_{L_i}$, we need to know the compressive strength, $\langle\sigma\rangle_{L_0}$, of a fiber that has a gauge length $L_0$, and the Weibull shape parameter of the (compressive) strength distribution, $\beta$. The dependence on the undercooling level, $\Delta T$, rather than on the stress level, $\langle\sigma\rangle_{L_i}$, is established by means of the model described in the theoretical section: for a given value of the undercooling, one calculates the residual thermal stress in the fiber, from which the number of breaks can then be derived (*via* Eq. 17). Prandy and Hahn[11] give, for a pitch-based HM carbon fiber with $L_0 = 10\,\text{mm}$, a compressive strength of $\langle\sigma\rangle_{L_0} \approx 1.08\,\text{GPa}$. As seen from Figure 7, inserting the latter together with a value of $\beta = 2$ into Eq. (17), yields, for the number of breaks per unit length, a range of values similar to the range of observed values (5 to 9 breaks per mm, as seen from Fig. 6), at $\Delta T = -130°\text{C}$. For comparison, $\beta = 4$ yields excessively high values of the number of induced breaks.

The experimental data relative to the fiber volume fraction may be used to predict the compressive Weibull shape parameter of the fiber. Using again the data of Prandy and

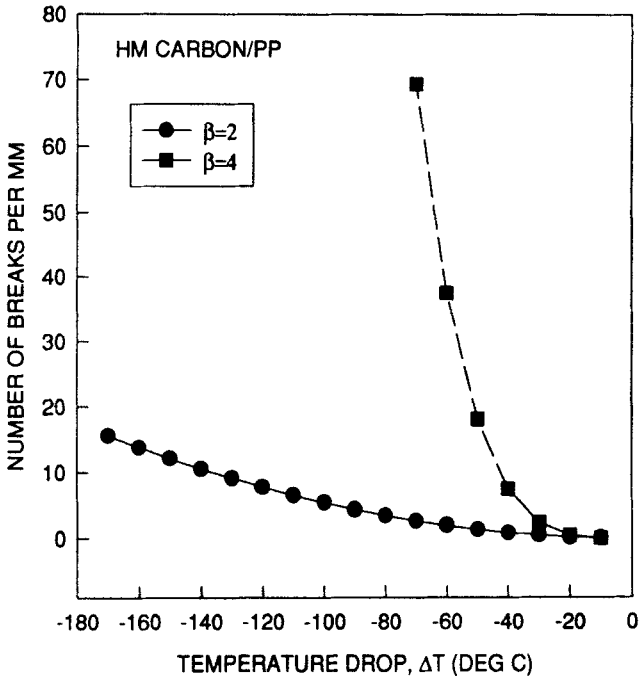


FIGURE 7 Predicted number of breaks per unit length of fiber as a function of temperature drop for HM carbon fibers in a polypropylene matrix, using two values of the compressive Weibull shape parameter of the fiber ($\beta = 2$ and 4).



Hahn[11] for 10 mm long HM and MM pitch-based carbon fibers, we have $\langle\sigma\rangle_{L_o} \approx 1.08$ GPa and $\langle\sigma\rangle_{L_o} \approx 1.8$ GPa, respectively. For each of the fiber volume fractions used in the experiment, at $\Delta T = -130°C$ and $\Delta T = -400°C$, respectively, theoretical values of the thermal residual stresses induced in the fiber, $\langle\sigma\rangle_{L_i}$, are calculated. These predicted stresses may then be substituted into Eq. (17), for several values of $\beta$, and compared with the experimental data as in Figures 8a and 8b. Such comparison yields the values of $\beta \approx 1.6$ for the HM carbon fiber and $\beta \approx 1 - 1.2$ for the MM carbon fiber.

### 4.2 Effect of a Transcrystalline Interlayer on Residual Stresses

The theoretical model presented in Section 3 enables the calculation of the predicted effect of a transversely isotropic transcrystalline interlayer upon the residual stresses in the fiber, the interphase and the matrix. We are particularly interested in the effect of the thickness of the interlayer upon the fiber axial compressive stress. The parameters needed in the theoretical analysis are the axial and radial Young's moduli ($E_z$ and $E_r$), the Poisson ratios ($\nu_{zr}$ and $J_{\theta r}$), the thermal expansion coefficients ($\alpha_z$ and $\alpha_r$) for all three components, the Weibull shape parameter of the fiber ($\beta$), $L_0$ and $\langle\sigma\rangle_{L_o}$, and $R_1$ and $R_3$. A simple spreadsheet program was written to calculate repeatedly and plot the fiber stress and the break density as a function of the thickness of the transcrystalline layer. Two cases were selected, as described in Table I, where both Young's moduli of the

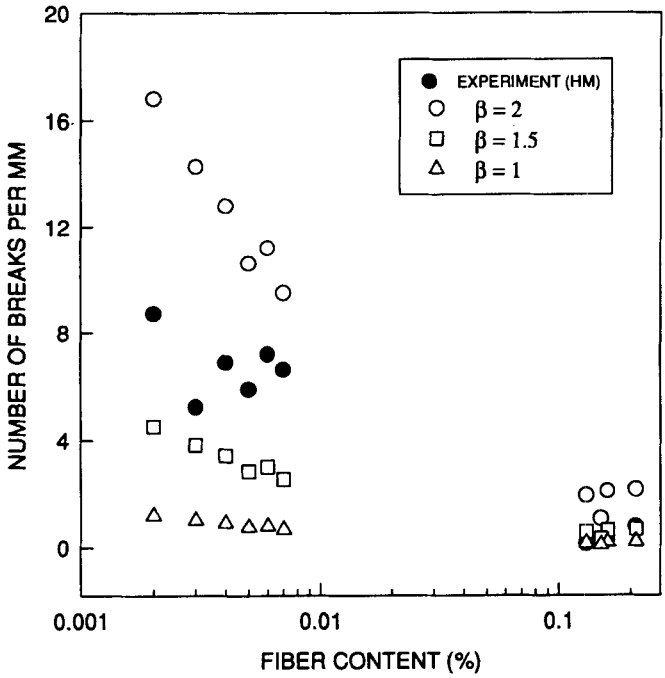


FIGURE 8a Best fit for the compressive Weibull shape parameter for HM carbon fibers in a polypropylene matrix, by comparison between calculated and experimental data for the number of breaks per unit length of fiber as a function of fiber volume fraction.



interlayer are larger than that of spherulitic polypropylene, but in Case 1 $E_z > E_r$, whereas in Case 2 the reverse is true. Note that these two cases might possibly correspond to different transcystalline morphologies. In both cases, the thermal expansion coefficients of the interlayer were smaller than that of spherulitic polypropylene. The model does not seem to be very sensitive to the values of the Poisson's ratios.

The theoretical predictions are presented in Figure 9. The difference between Case 1 and Case 2 is striking. It appears that if $E_z > E_r$ then the fragment length increases (or the compressive stress in the fiber decreases) with progressively thicker interfaces, whereas if $E_z < E_r$ the fragment length (or the compressive fiber stress) is insensitive to the thickness of the transcrystalline zone. However, the trend of the experimental results presented in Figure 9 seems to differ strongly from the theoretical prediction: as seen, the average fiber fragment length seems to decrease rapidly (within a distance of 20 μm) in the presence of a transcrystalline layer towards a fragment length plateau value of about 130 μm. A similar trend was recently obtained by Klein and Marom[12] using pitch-based HM carbon fiber/Nylon-66 matrix composite. However, experimental results differing from those presented here, and from those of Klein and Marom[12] with HM carbon/Nylon-66, were earlier obtained by Incardona *et al.*[14] using HM carbon/J-polymer and, more recently, by Wood *et al.*[15] using HM carbon/polycarbon-

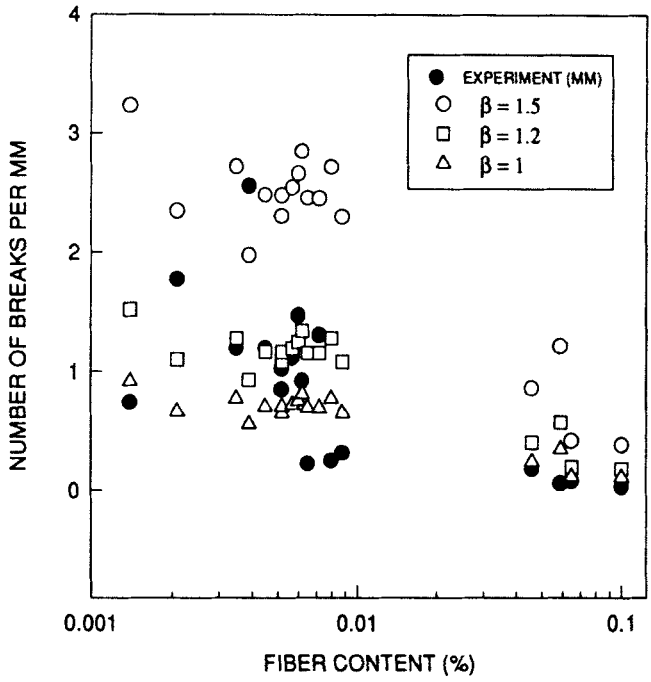


FIGURE 8b Best fit for the compressive Weibull shape parameter for MM carbon fibers in a polypropylene matrix, by comparison between calculated and experimental data for the number of breaks per unit length of fiber as a function of fiber volume fraction.



ate. These authors found that the average fiber fragment length progressively increases with the interlayer thickness, similar to our theoretical predictions in Figure 9 at the condition that $E_z > E_r$ (Case 1, Fig. 9).

Before the discussion on the effect of the interlayer thickness is further expanded, we present data from a cooling rate experiment, which apparently confirm the trend of the experimental data in Figure 9 (and contradict the theoretical trend of Case 1): At very slow (0.3°C $min^{-1}$) and very fast (400°C $min^{-1}$) cooling rates, no transcrystals are observed, and relatively larger fragments are observed (Fig. 10). At intermediate cooling rates, transcrystalline layers are observed and, at the same time, the average fragment length decreases. Figure 11 shows the effect of cooling rate on the morphology. One can observe the different morphologies surrounding the fiber (note also the large and small spherulites, and no transcrystalline layer, at extreme cooling rates). Thomason and Van Rooyen[13] suggest that transcrystallization is caused by stresses at the fiber-melt interface due to mismatch in the thermal expansion coefficients of the fiber and the matrix and, further, that the occurrence of transcrystallization is dependent on the cooling rate. Our findings support their assertion, at least for slow and intermediate cooling rates, as well as their observation that below a cut-off cooling rate-which depends on the fiber substrate-no transcrystallinity is obtained.

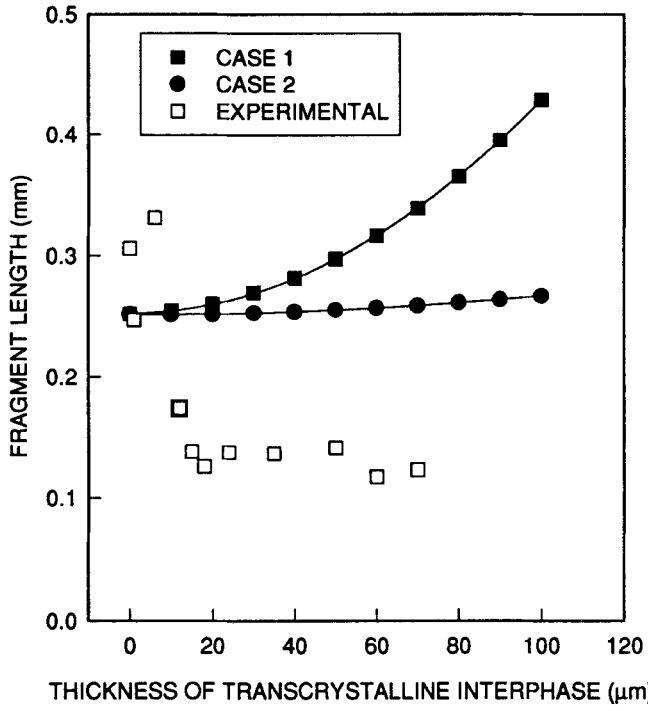


FIGURE 9 Comparison between theoretical prediction and experimental data for the fiber fragment length as a function of the thickness of the transcrystalline interlayer, using HM carbon fibers in a polypropylene matrix. Refer to Table I for relevant thermoelastic data used in the calculation. Also included in the calculation were the following parameters: $\beta = 1.6$, $L_0 = 10\,\text{mm}$, $\langle\sigma\rangle_{L_0} = -1.08\,\text{GPa}$, $\Delta T = -130^\circ\text{C}$.



We now address the question as to why is the experimental trend of the data in Figure 9 opposite to the predicted trend? Three points can be made:

(1) The actual value of $\Delta T$ may be different when growing a thin or a thick transcrystalline interlayer isothermally, whereas the theoretical model assumes the same value of $\Delta T$ in both cases. Indeed, a thin interlayer is grown by leaving the specimen for a relatively short time at the isotherm, then fast cooling it to, say, 0°C, whereas growing a thick interlayer necessitates much longer times before fast cooling. When a thin interlayer is grown, and fast cooling performed, most of the surrounding bulk matrix is still in the molten state and solidification starts, in fact, at a temperature that is lower than the isotherm, giving rise to a smaller value of $\Delta T$, thus to smaller residual stresses and less fiber breaks, or longer fiber fragments. On the contrary, most of the surrounding bulk matrix is already solid when a thick interlayer is grown at the same isotherm, giving a larger value of $\Delta T$ and larger residual stresses, and thus more fiber breaks and shorter fragments. This might constitute a partial explanation for the experimental trend in Figure 9.

(2) As mentionned above, during the growth of the transcrystalline interlayer at an isothermal temperature, there is, in parallel, progressive crystallisation of the

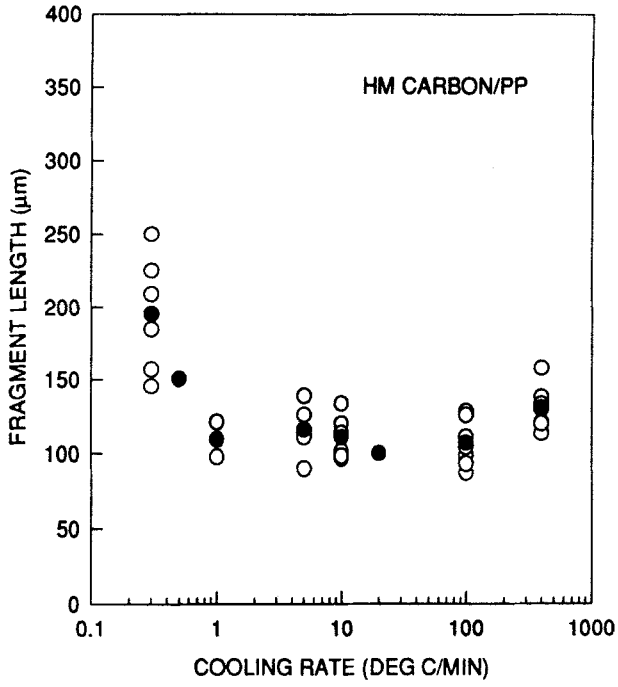


FIGURE 10 Effect of cooling rate on the fragment length in pitch-based HM carbon fibers embedded in a polypropylene matrix. The full circle symbol (●) represents the average value.



bulk polypropylene matrix surrounding the transcrystalline interlayer and the fiber. Since the time required to grow a transcrystalline interlayer of a particular thickness also has a strong effect on the properties of the spherulitic matrix, the degree of crystallinity, and hence the thermoelastic properties, of the bulk matrix will be different for samples with different transcrystalline layer thicknesses. Thus, a comparison of experimental results at various transcrystalline thicknesses as presented in Figure 9 hardly reveals the true, isolated, effect of a transcrystalline interlayer. In fact, Wood *et al.*[15] found that by growing a transcrystalline phase of polycarbonate at the surface of a carbon fiber without any apparent change in the amorphous nature of the bulk matrix, the thermal residual stresses in the fiber decreased, and the fragment length increased, confirming the theoretical predictions in Figure 9 at the condition that $E_z > E_r$ (Case 1, Fig. 9). Note that, alternatively, if the properties of the bulk matrix progressively vary with thickening transcrystalline interlayers, it should be possible to apply repeatedly the theoretical model to assess whether the fragment length decreases with interlayer thickness, similar to the experimental data in Figure 9.

(3) One should be cautious in applying the above theoretical models, since the various thermoelastic constants (Young's moduli, Poisson's ratios, thermal expansion coefficients) are affected by temperature (and possibly by the cooling rate). Moreover, remembering that the fiber is subjected to compressive stresses,

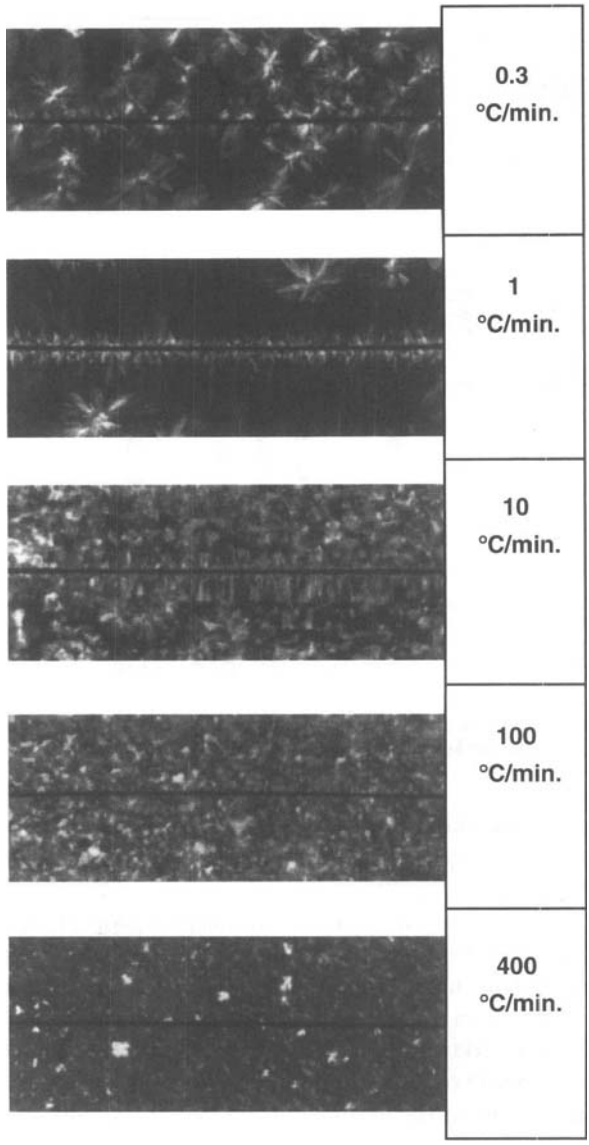


FIGURE 11 Matrix morphology around HM carbon fiber in a polypropylene matrix, cooled at various rates from the melt to room temperature. (See Color Plate III).

the *compressive* values of its elastic constants (which may differ from their tensile counterparts) should be used.

Regarding the transcrystalline interlayer in particular, no direct experimental measurements of the thermoelastic constants are yet available, and only rough estimates can be made for these, as we have done in Figure 9, to predict the observed trends.

## 5. CONCLUSIONS

We have shown that it is possible to measure certain mechanical properties of single fibers in compression, by means of the fiber fragmentation phenomena resulting from compressive residual thermal stresses. The residual thermal stresses present in the fiber, and the related average fiber fragment lengths, can be predicted by means of a concentric three-cylinder model in which the cylinders are transversely isotropic. The effect of fiber volume fraction on the residual thermal stresses in the fiber was also measured and compared with the theoretical predictions. An estimated value of the Weibull shape parameters of HM and MM carbon fibers in compression was derived from the combined theoretical predictions and experimental measurements.

The effect of the thickness of the transcrystalline layer on the average fiber fragment length due to compression was also investigated. Experimental data apparently show that thicker transcrystalline interlayers induce higher residual stresses in the fiber, leading to shorter fiber fragments. This result is backed up by cooling rate experiments where no transcrystalline layer can be grown at the two extreme cooling rates of 400°C $min^{-1}$ and 0.3°C $min^{-1}$, for which a large fiber fragment length is observed, contrasting with intermediate cooling rate tests for which a transcrystalline layer is observed and smaller fragment lengths obtained. Theoretical predictions show that (i) the opposite should occur (less residual stress–or longer fragments–in the fiber in the presence of thicker transcrystalline layers) if $E_z > E_r$ where $E$ designates the modulus of the interlayer, or (ii) the interlayer has almost no effect on the fiber residual stress if $E_z < E_r$. Reasonable causes for the conflicting results arising from theory and experiments were presented. Moreover, recently published results with an amorphous polycarbonate matrix surrounding a transcrystalline region grown on a carbon fiber seem to confirm the theoretical prediction. As a final conclusion, direct experimental measurements of the thermoelastic constants for the various types of transcrystalline interlayers, as well as a detailed study of the related transcrystalline morphologies, would provide a more definite answer to some of the questions raised in the present study.



### Acknowledgements

This research was supported by the Basic Research Foundation administered by the Israel Academy of Sciences and Humanities. Stimulating discussions with G. Marom and J. Wood are acknowledged.

### References

1. H. D. Wagner and A. Eitan, *Applied Physics Letters*, **56,** 1965 (1990).
2. H. E. Gallis, B. Yavin, J. Scherf, A. Eitan and H. D. Wagner, *Polymer Composites*, **12,** 436 (1991).
3. A. Kelly and W. R. Tyson, *J. Mechanics Physics Solids*, **13,** 329 (1965).
4. H. L. Cox, *Brit. J. Appl. Physics*, **3,** 72 (1952).
5. J. A. Nairn, *Polymer Composites*, **6,** 123 (1985).
6. H. D. Wagner *Composite Interfaces*, in press (1995).
7. H. D. Wagner, *J. Adhesion*, **52,** 131 (1995).
8. H. D. Wagner, Submitted (1995).
9. S. G. Lekhnitskii, *Theory of Elasticity of an Anisotropic Elastic Body* (Holden-Day, San Francisco, 1963), p. 66.
10. H. D. Wagner, J. R. Wood and G. Marom, *Advanced Composite Letters*, **2,** 172 (1993).
11. J. M. Prandy and H. T. Hahn, *SAMPE Quarterly*, **22,** 47 (1991).

12. N. Klein, G. Marom, The Hebrew University of Jerusalem, private communication (1994).
13. J. L. Thomason, A. A. Van Rooyen, *J. Mater. Sci.*, **27,** 897 (1992).
14. S. Incardona, C. Migliaresi, H. D. Wagner, A. H. Gilbert and G. Marom, *Composites Sci. and Technol.*, **47,** 43 (1993).
15. J. R. Wood, H. D. Wagner, G. Marom, *J. Mater. Sci. Letts.*, in press (1995).